UNIVERSIDAD NACIONAL DE COLOMBIA

Geología Colombiana, 2015 - Vol. 40

MAPPING IRON BEARING FORMATION USING HYPERSPECTRAL AND MULTISPECTRAL IMAGES. A CASE STUDY OF SINGHBHUM - KEONJHAR IRON BELT - INDIA

MAPA DE FORMACIÓN DEL DEPOSITO DE HIERRO UTILIZANDO LAS IMÁGENES HIPERSPECTRALES Y MULTISPECTRALES. UN ESTUDIO DE CASO DE SINGHBHUM - KEONJHAR IRON BELT - INDIA

Jhonny José Herrera García Geólogo

interjhonny@gmail.com

Autor's Address: Calle Juan González N35-73 y Juan pablo Sanz. Edif. Normandía
Piso 6. Dpto. 604. Telephone: +593 958999757

Herrera G., J., J., (2015): *Mapping Iron Bearing Formation Using Hyperspectral and Multispectral Images. A Case Study of Singhbhum - Keonjhar Iron Belt - India*.- GEOLOGIA COLOMBIANA, Vol. 40. Bogotá, Colombia D.C.. pp. 61-78

Manuscrito recibido: 15 de Octubre de 2015; aceptado: 6 de Diciembre de 2015

Resumen

Las imágenes hiperespectrales entre los sensores remotos, se han utilizado durante más de una década para ayudar en la detección e identificación de diversos objetivos de superficie como características topográficas y geológicas, pero los conjuntos de datos no son inmunes a los efectos de la atmósfera intermedia. Varios constituyentes atmosféricos atenúan la reflectancia incidente y ascendente, y finalmente degradan la señal correspondiente a la característica detectada. Por lo tanto, si esta atenuación atmosférica pudiera identificarse y corregirse utilizando modelos de transferencia radiativa existentes, sería posible una mejor comprensión de las características de la Tierra.

El presente estudio se concentra en la recuperación de la imagen de reflectancia a partir del nivel uno corregido radiométricamente, de los datos del área de estudio del distrito de Keonjhar (Orissa). En este estudio, se ha utilizado un modelo de corrección atmosférica, conocido como **FLAASH,** que se ha utilizado para recuperar la imagen de reflectancia a partir de los datos de radiancia. El pre-procesamiento del conjunto de datos debe realizarse antes de aplicar la corrección atmosférica en el conjunto de datos. Los subconjuntos espectrales de las bandas propensas al ruido se han realizado con éxito, lo que deja 196 bandas exclusivas de 242 bandas del conjunto de datos de Hyperion. Se recolectaron tres miembros finales del área de estudio de Orissa: La hematita; los relaves mineros; y el aluvión, que se seleccionaron como los miembros finales después de comprender la geología y el análisis de la imagen de reflectancia.

En este sentido se aplicaron: La desmezcla espectral lineal y el Mapeador de ángulo espectral. En el área de estudio, Lineal Spectral Unmixing (LSU), dio buenos resultados en el mapeo de los miembros finales. El procesamiento de imágenes se llevó a cabo con datos digitales Landsat - 5TM (7 bandas) adquiridos el 5 de noviembre de 2005 (ruta 140, fila 45). El objetivo de este estudio fue mapear las zonas más favorables de la Formación del depósito de hierro dentro de la conocida franja mineralizada, además de identificar y mapear las extensiones de mineralización conocida y/o localizar las nuevas zonas potencialmente mineralizadas que son ricas en mineral de Hierro.

Palabras clave: *Hiperespectral, Hyperión, Landsat, Multiespectral, Keonjhar, Mineral de hierro.*

Abstract

Hyperspectral imaging sensors have been used for more than a decade to aid in the detection and identification of diverse surface targets, topographical and geological features, but the datasets are not immune to the effects of the intervening atmosphere. Various atmospheric constituents attenuate the incident and up-welling reflectance and finally degrade the signal corresponding to the feature being sensed. Thus, if this atmospheric attenuation could be identified and corrected for by using existing radiative transfer models, better understanding of the earth features would be possible.

The present study concentrate on the retrieval of reflectance image from the level one radiometrically corrected data of study area of Keonjhar district (Orissa). In this study, one atmospheric correction model has been used. FLAASH atmospheric correction model have been used to retrieve reflectance image from the radiance data. Preprocessing of the dataset, need to be done before applying atmospheric correction on the dataset. Spectral sub-settings of noise prone bands have been successfully done which leaves 196 unique bands from 242 bands of the Hyperion dataset. Three endmembers were collected from the Orissa study area; Hematite, mine tailings and alluvium were selected as the endmembers after understanding the geology and analysis of the reflectance image. Linear Spectral Unmixing and Spectral Angle Mapper were applied in this regard. In the study area, Linear Spectral Unmixing gave good results in mapping the endmembers. In the present study, image processing was carried out to a Landsat - 5 TM digital data (7 bands) acquired on 05-November-2005 (path-140, row-45). The aim of this study was mapping the more favorable zones of Iron Bearing Formation within the known mineralized belt, besides to identify and map the extensions of the known mineralized and/or to locate the new potentially mineralized zones which are rich in Iron ore.

Keywords: *Hyperspectral, Hyperion, Landsat, Multispectral, Keonjhar, Iron ore.*

INTRODUCTION

One of the most common techniques that are very much useful in mineral exploration prospecting is the Remote Sensing. The term remote sensing can be defined as the science of acquiring, processing, and interpreting images that record the interaction between the electromagnetic energy and matter (Sabins, 1996).

One of the most promising and advanced remote sensing technique which is meant solely for mineral exploration is Hyperspectral Remote Sensing or otherwise known as Imaging Spectrometry. Imaging spectroscopy is a relatively new technology that is currently being investigated by researchers and scientists with regard to the detection and identification of minerals, terrestrial vegetation, and man-made materials and backgrounds. The concept of hyperspectral remote sensing began in the mid-80 and to this point has been used most widely by geologists for the mapping of minerals. Actual detection of materials is dependent on the spectral coverage, spectral resolution, and signal-to-noise of the spectrometer, the abundance of the material and the strength of absorption features for that material in the wavelength region measured (source: http://www.csr.utexas.edu/ projects/rs/hrs/hyper.html).

Imaging spectrometers typically acquire images in a large number of spectral bands (more than 100). These bands are narrow (less than 10 nm to 20 nm in width), and contiguous (i.e. adjacent), which enables the extraction of reflectance spectra at pixel scale. Such narrow spectra enable the detection of the diagnostic absorption features which are not represented or manifested by the multispectral sensors when light interacts with a mineral or rock. The objectives of these hyperspectral imaging spectrometers are to use the molecular absorptions and constituent scattering characteristics expressed in the spectrum to (1) detect and identify the surface and atmospheric constituents present; (2) assess and measure the expressed constituent concentrations; (3) assign proportions to constituents in mixed spatial elements; (4) delineate spatial distribution of the constituents; (5) monitor changes in constituents through periodic data acquisitions; and (6) to validate, constrain and improve models (Pantazis *et al*., 1998). With the aid of hyperspectral remote sensing, an extensive range of minerals can be remotely mapped, including iron oxides, clays, micas, chlorites, amphiboles, talc, serpentines, carbonates, quartz, garnets, pyroxenes, feldspars and sulphates, as well as their physico-chemistries such as the cation composition and long and short range order (Cudahy, 2002).

Another remote sensing technique widely used in the past decades to discriminate different materials based on the dissimilarity that exist among their spectral properties is the multispectral remote sensing (Hunt *et al.,* 1971). Geological applications could greatly take advantage of this technology because it allows observing and mapping the surface of the Earth over large areas, but the generally low spectral resolution of multispectral sensors obstruct geological research.

In the present study, image processing was carried out to a Landsat TM - 5 digital data (7 bands) acquired on 05-November-2005 (path-140, row-45). Different image processing techniques were applied to this image using the ERDAS software like Ratio transformations and PC transformations.

STUDY AREA

The Hyperion and Landsat TM scenes include the Keonjhar District (Orissa), which has been the study area selected for the present study. The study area has been chosen for the present study keeping in mind the topography. Keonjhar District (Orissa) is a densely vegetated terrain with large number of hillocks and dissected hills spread out throughout the valley. Geologically the region comes under the Pre-Cambrian era of the geological time scale.

Orissa state is well covered by the Hyperion and Landsat TM scenes. The selected project area includes the south-eastern margin of the famous Iron Ore Super Group Syncline, mainly consisting of iron ore group, is bounded by latitude 21º 45' to 22º 00' N and longitude 85º 15' to 85º 30' E occupying an area of approximately 770 sq. Km **(Figure 2.1).** To the north of this area are the main townships of Joda, Barbil, Noamundi, Bolani, Kiriburu, Meghahatuburu and so many other mining centers of Fe and Mn, ores. Most of the above mentioned towns are connected by railway and roadways routes to Jamshedpur, Rourkela, Keonjhar, Chaibasa and Bhubaneshwar. The area under the present study is unfortunately not provided with easily motorable road except north eastern and north-western parts, (Figure 1).

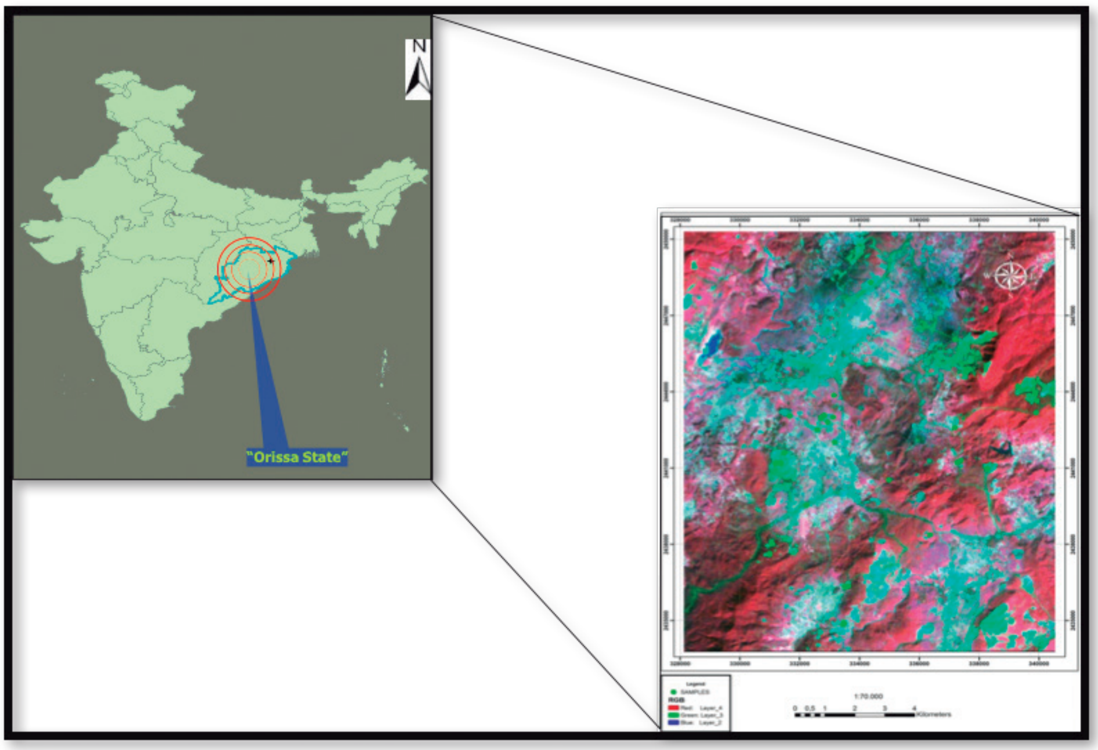

Figure 1. - Study area Keonjhar District (Orissa), Landsat TM - 5 (Bands 4 3 2).

METHODOLOGY

The methodology for the present study has been formulated by keeping in mind the primary objectives of the work. During the literature review for the present study it came to the limelight that very few works have been conducted in the field of hyperspectral remote sensing in India which could assist our efforts for the present study. The methodology adopted for the present study is given below as a flow chart, (Figure 2).

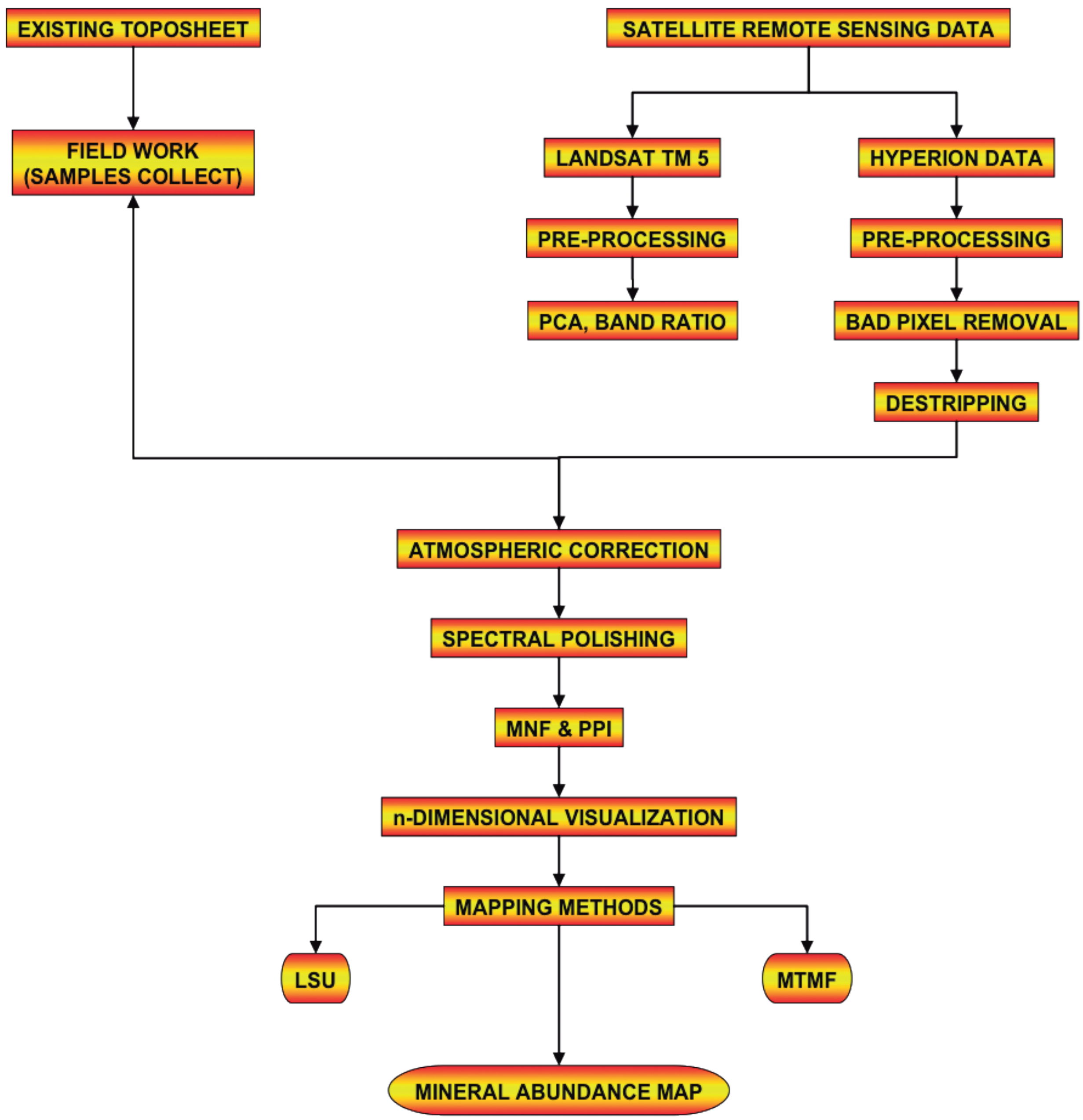

Figure 2. - Methodology flow chart for the present study.

RESULT AND DISCUSSIONS

RATIO 3/1

In the ratio of Landsat TM–5 of band 3 and band 1 (3/1), the most of the area in bright pixels, corresponds to zones of strong hematitic alteration (Figure 4.3). The Spectral response of the weathered iron minerals has weak reflectance in the blue region (band 1) and strong reflectance in the red region (band 3), so the ratio 3/1, which has high values can be used for iron oxide mapping in Orissa area (Figure 3).

RATIO 5/7

The 5/7 ratio has been useful for identifying clay-rich rocks (dark gray-tones) because clay minerals exhibit strong absorption in the 2.2 µm region (band 7) and high reflectance in the 1.6 µm region besides this ratio is useful for Iron minerals because this have reflectance and absorptions features in these bands (Hunt *et al.* 1971) (Figure 4).

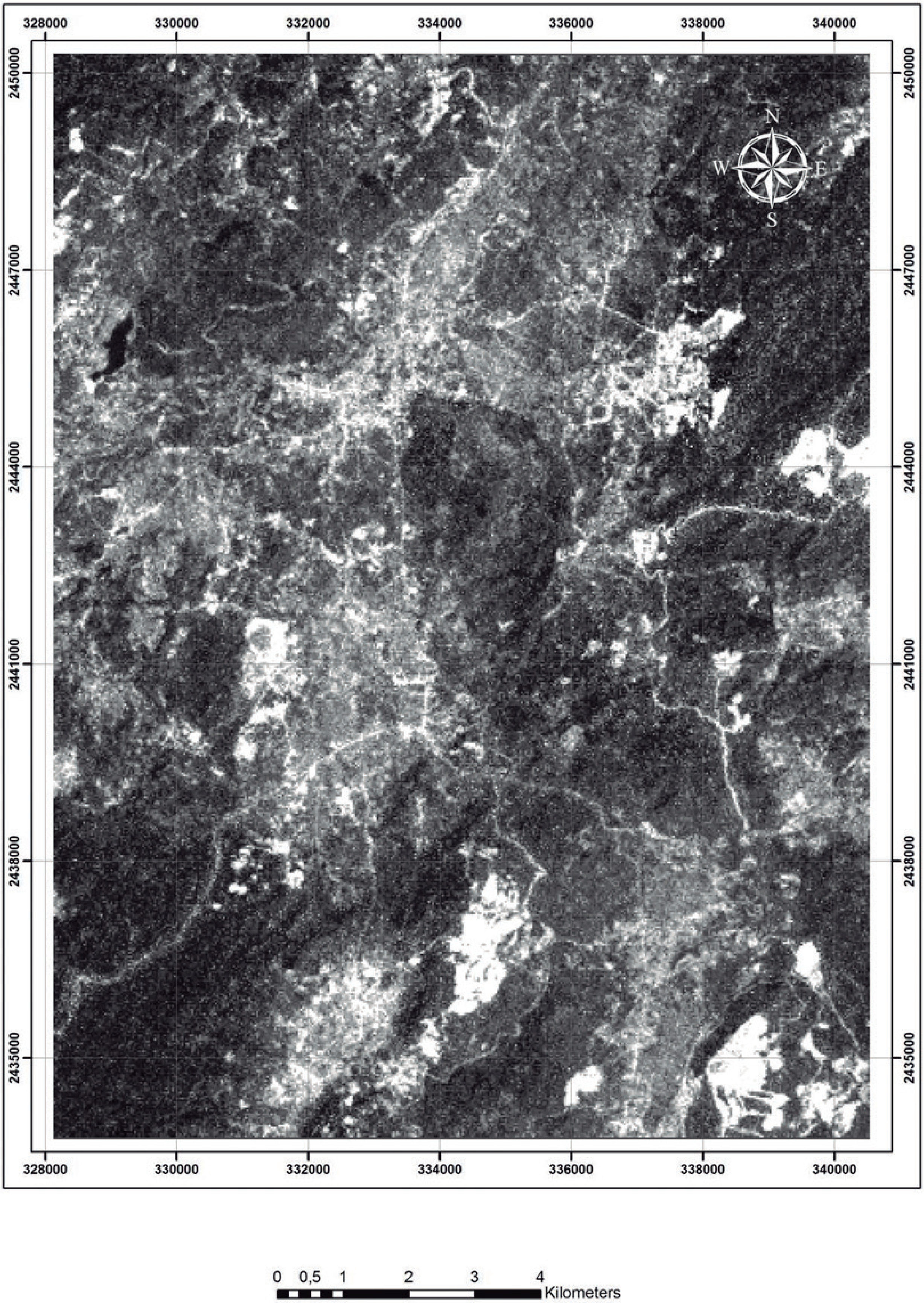

Figure 3. - TM band ratio 3/1.

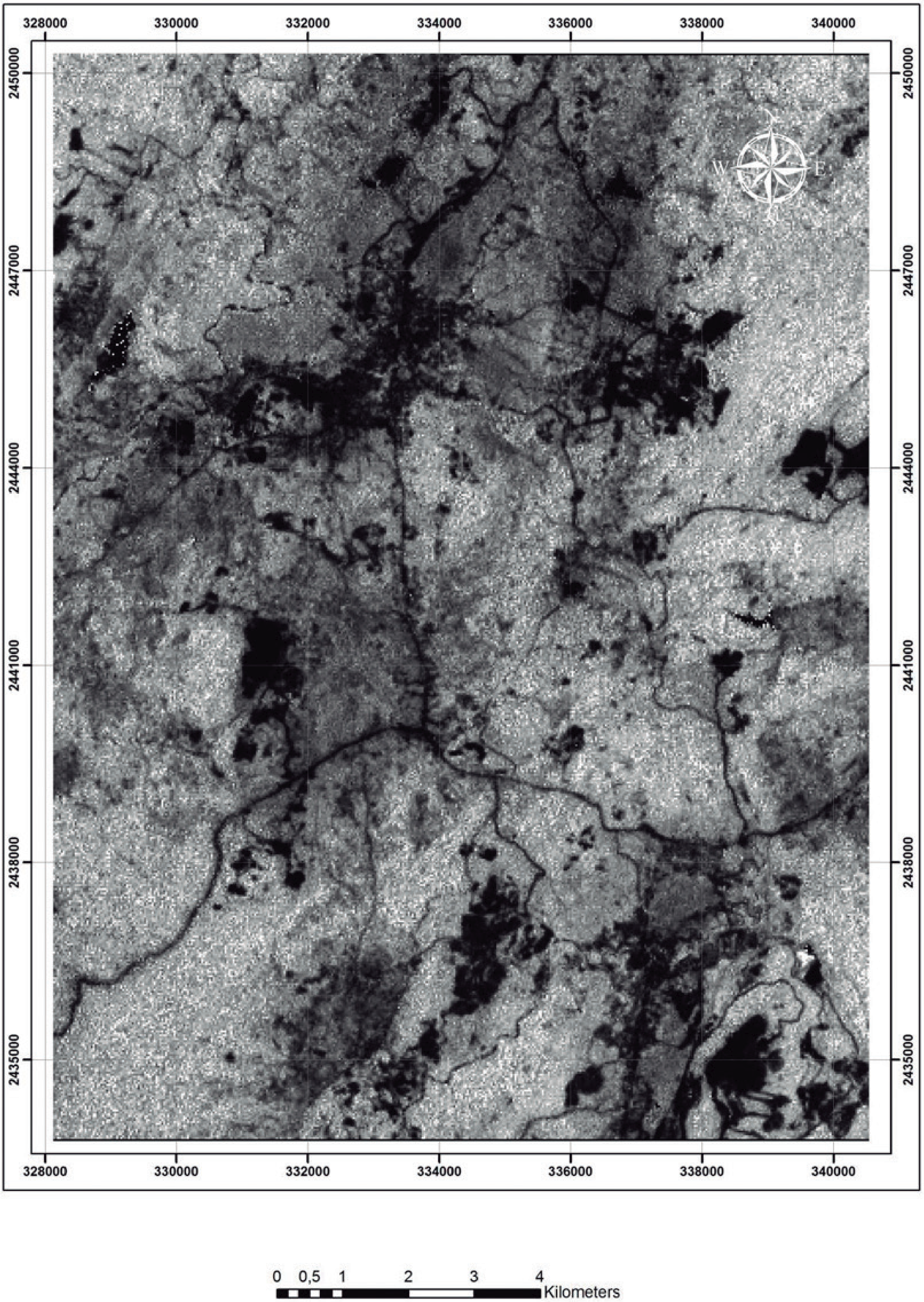

Figure 4. - TM band ratio 5/7.

RATIO 5/4

The ratio of Landsat TM – 5 of band 5 and band 4 (5/4), has been computed to enhance possible ferrous oxides because this ratio shows higher values for oxidized iron-rich rocks than other types (Figure 5).

Based on the above considerations, the spectral features of ferric and hydroxyl – bearing mineral are used to produce a false colour composite image using combinations of ratio 5/7, 5/4 and 3/1 in R, G and B respectively. The obtained image has mapped the bearing mineral zone (Ferric Zones) in bluish. These zones can easily be observed in the lower right corner, central and right central part of the image (Figure 6). Another composite image was produced using ratio 3/1, PC2 and Band 7 in R, G and B respectively. Although this combination of ratio image appears to be fairly different from the previous one, the final result remains the same thus lending support to the previous conclusion. The dark red represents the zones of strong hematitic alteration (Figure 7).

PRINCIPAL COMPONENT ANALYSIS

Principal Components Analysis (PCA) can be used for image analysis as a data reduction technique that the information content from a number of bands is compressed into a few principal components. In other words, PCA can be used to reduce the dimensionality of the data while minimizing loss of information. In addition, PCA images may be more easily interpreted than the conventional color infrared composite. The principal components transform is a standard method for deriving a new set of images with reduced spectral redundancy. PCA is probably the oldest and best known of the techniques used for multivariate analysis. The overall goal of PCA is to reduce the dimensionality of data set, while simultaneously retaining the information present in the data. Here in the present study 6 haze corrected Landsat TM bands (3 in visible and 3 in reflected IR) were considered for calculation of principal components. The principal transformation (eigen vectors) using an input of six TM bands are shown in table 1.

Table 1. - Principal component analysis of six haze corrected TM bands of Orissa study area.

CORRELATION EIGENVECTORS	PC1	PC2	PC3	PC4	PC5	PC6	WAVELENGTH
BAND1	0,067	-0,024	-0,340	-0,006	0,409	-0,844	0,45 - 0,52
BAND2	0,131	-0,008	-0,591	-0,056	0,588	0,534	0,52 - 0,60
BAND3	0,213	-0,144	-0,676	0,051	-0,687	-0,040	0,63 - 0,69
BAND4	0,260	0,916	-0,042	0,299	-0,047	-0,013	0,76 - 0,90
BAND5	0,657	0,058	0,167	-0,732	-0,025	-0,024	1,55 - 1,75
BAND7	0,659	-0,369	0,221	0,607	0,109	0,022	2,08 - 2,35

It was observed in the table 1 that the first component (PC1) is all positive. This PC1 gives information mainly on albedo and topography (Figure 8.a). PC2 clearly discriminates the water bodies and mining areas as dark pixels (Figure 8.b). Analysis of PC3 shows that the most important contributions come from Band 5 (0.167) and Band 7 (0.221). Hydroxyl-bearing (clay) minerals image is obtained by using eigenvector loadings of PC3 (Figure 8.c). The similar analysis of PC4 shows that the most important contributions come from Band 4 (0,299), Band 5 (-0.732) and Band 7 (0.607). Based on spectral characteristics of iron oxide, it follows that iron oxide will be mapped by bright pixels and ferrous minerals in dark grey. Iron oxide image is obtained by using eigenvector loadings of PC4 (Figure 8.d). PC5 contains positive information from band 7 (0.109) and negative information from band 3 (-0.687) which should show the position of hydroxyl ions as dark-gray pixels (Figure 8.e). PC6 mostly shows noise in the dataset, limiting the use particular of this particular band in our analysis (Figure 8.f).

Based in the results obtained in the PC analysis, a false colour composite image was created using combinations of the PC4, PC3 and PC2 in R, G and B respectively. The obtained image has mapped the bearing mineral zone (Iron-bearing zones) in yellow and dark-green (Figure 9).

MINERAL ABUNDANCE MAP

Maximum Likehood Classifier was applied to the MNF transformed components, using the ROI’s of selected endmembers. In order to compare the results with those from the Maximum Likelihood, the classification thresholds are adjusted to 3. The **(Figure, 10)**, show the mineral abundance map created.

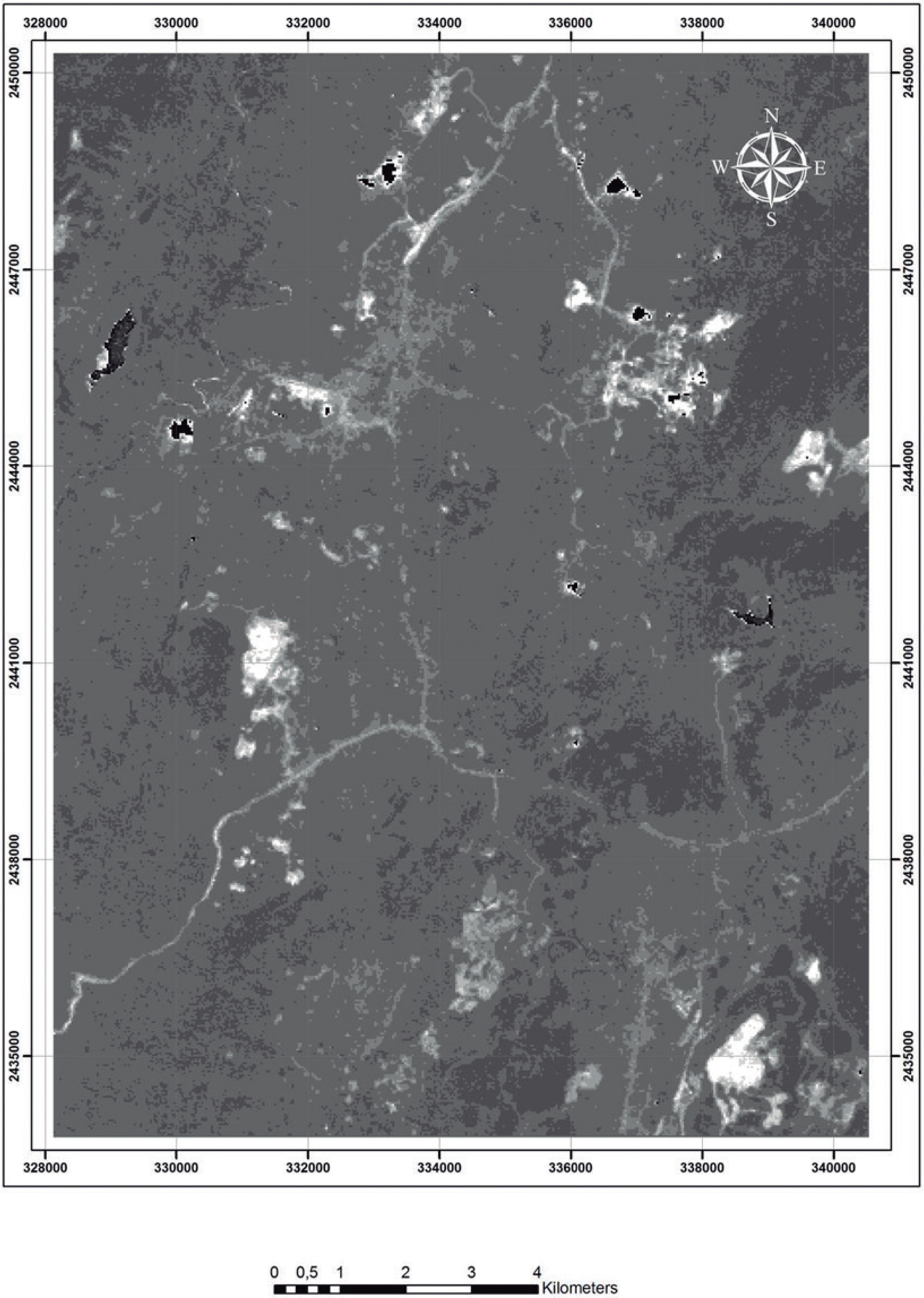

Figure 5. - TM band ratio 5/4.

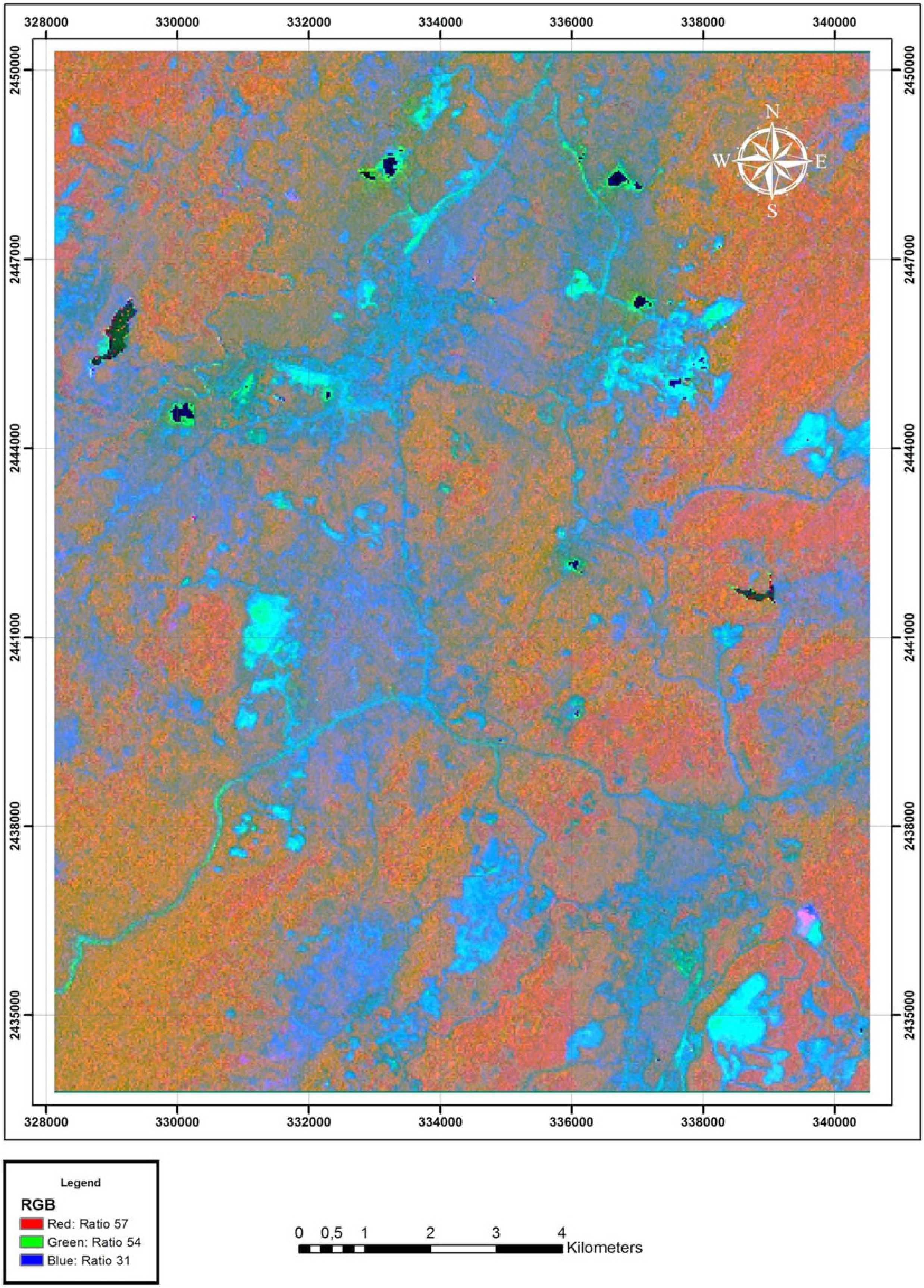

Figure 6. - Color composite of TM image. Ratio 5/7 (red), Ratio 5/4 (green), Ratio 3/1 (blue).

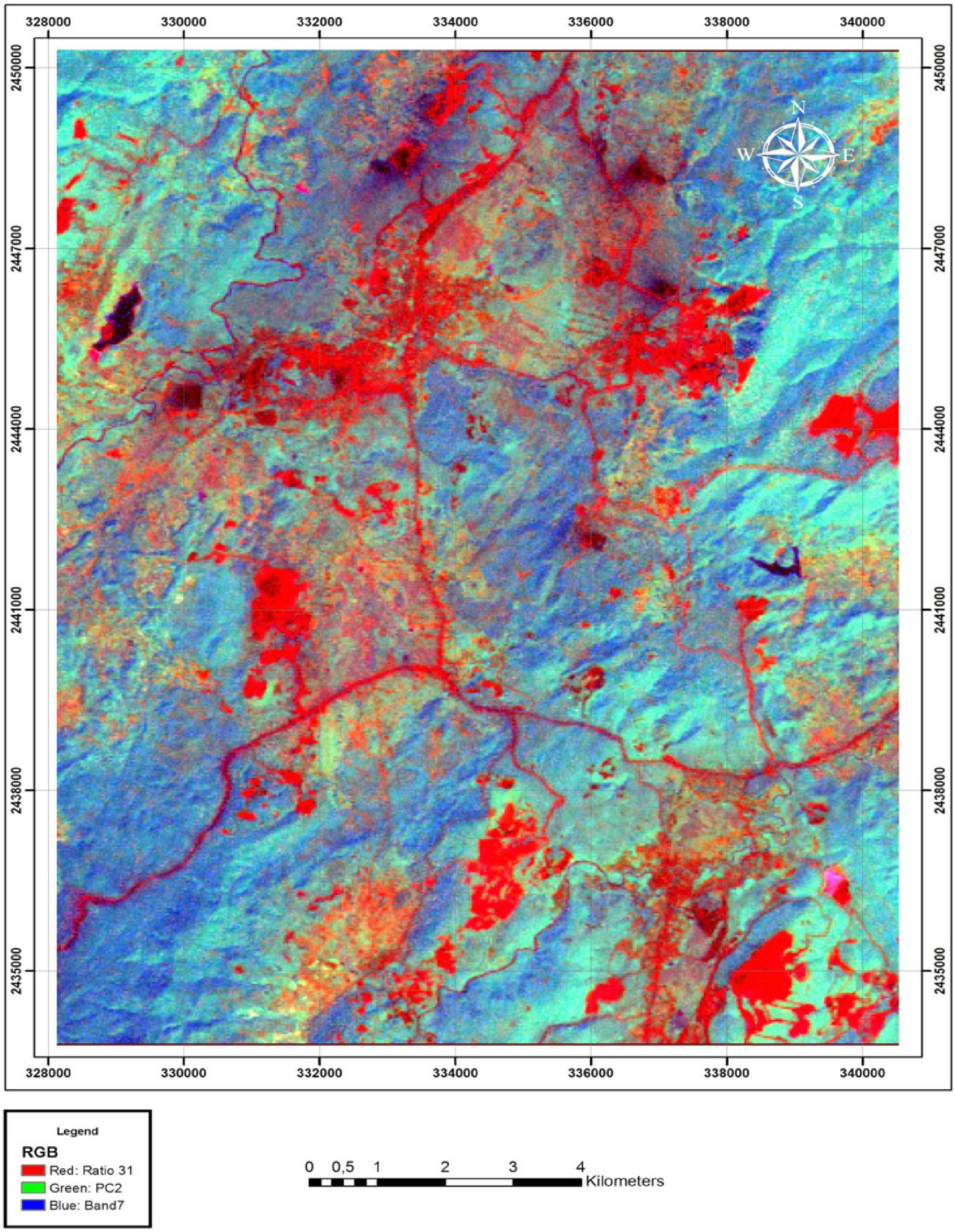

Figure 7. - Color composite of TM image. Ratio 3/1 (red), PC2 (green), Band 7 (blue).

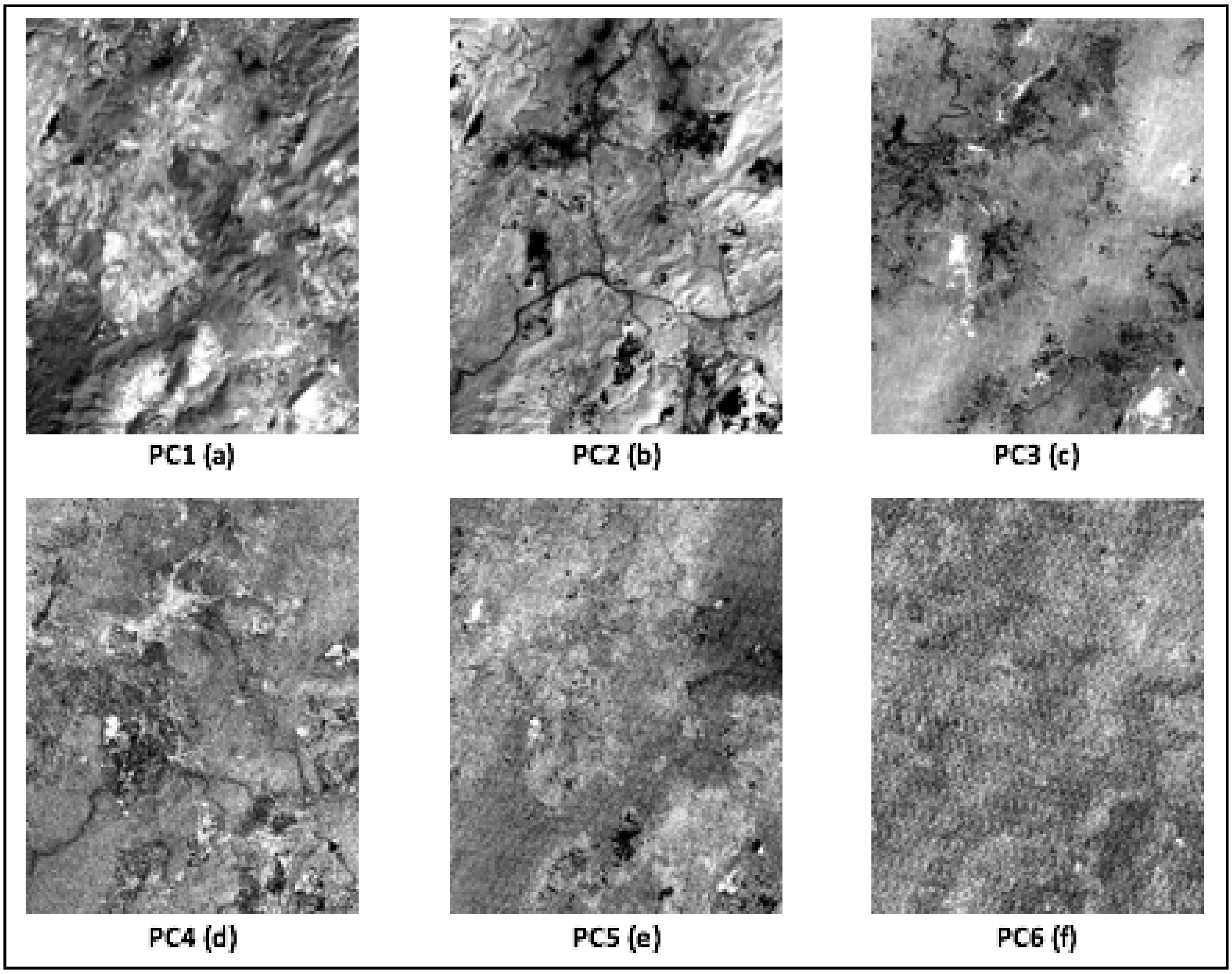

Figure 8. - Principal Components images showing spectral variability of the study area.

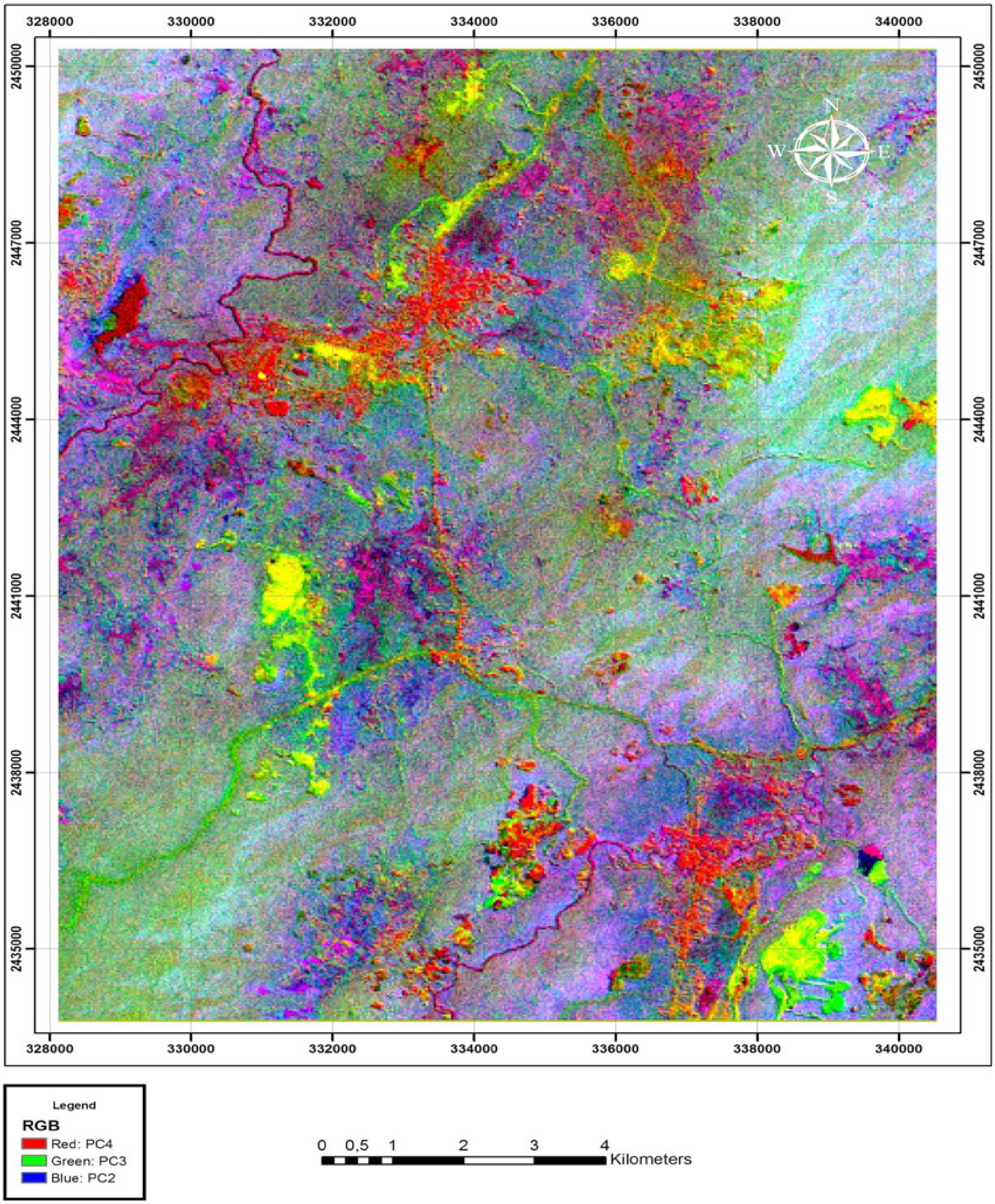

Figure 9. - Color composite of TM image. PC4 (red), PC3 (green), PC2 (blue).

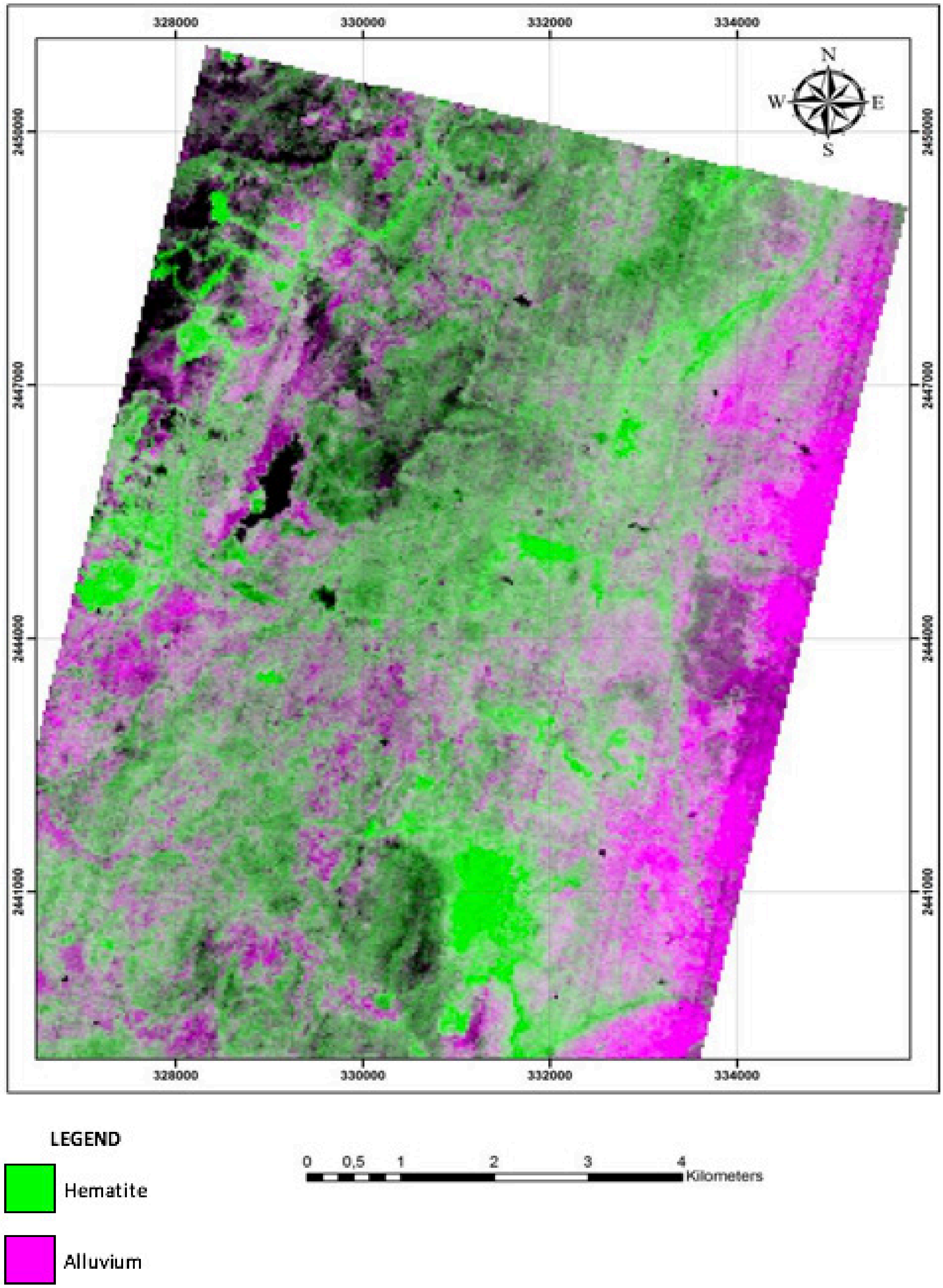

Figure 10. – Mineral Abundance Map.

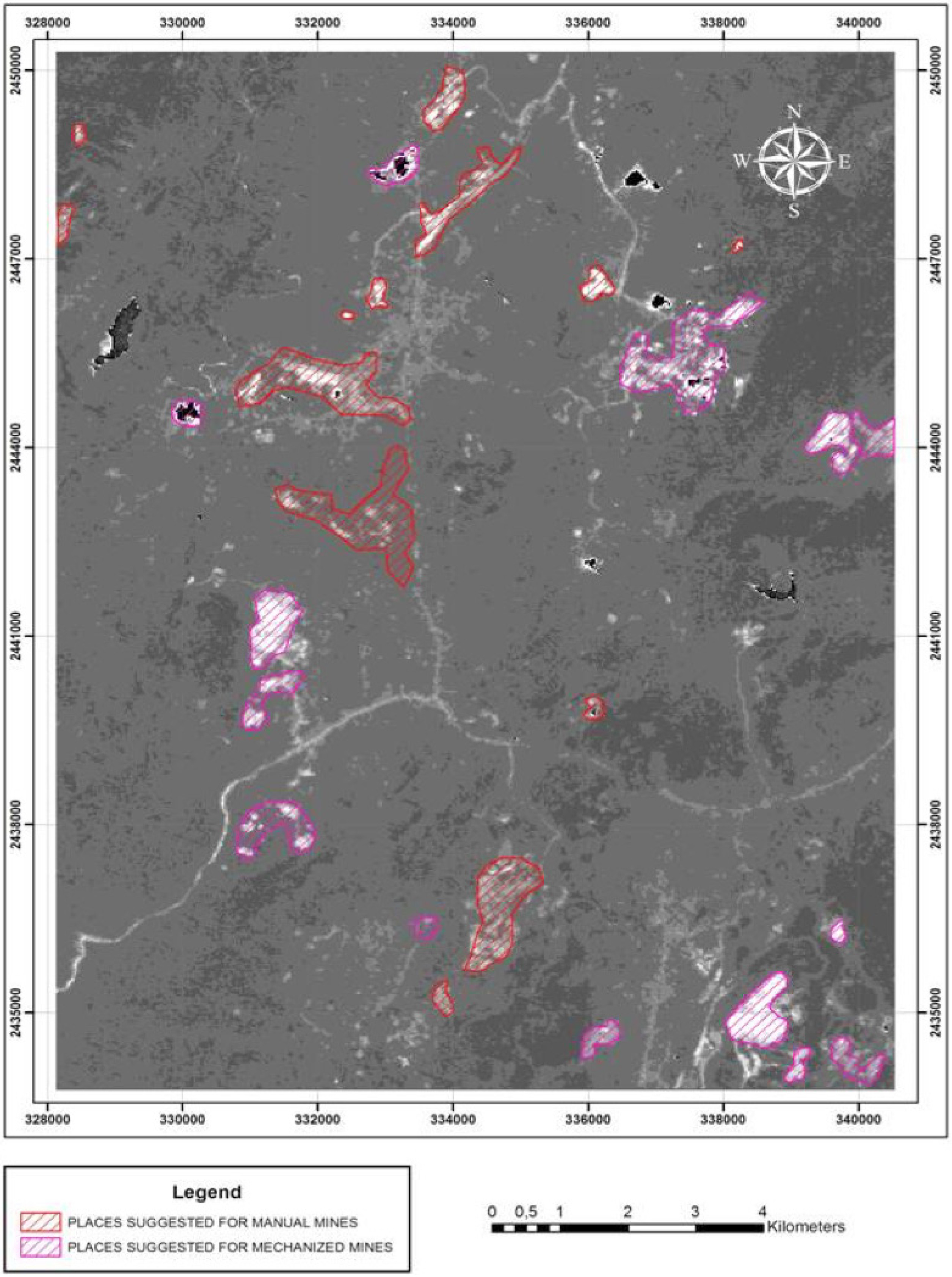

Figure 11. - More favorable zones of Iron Bearing Formation and potentially mineralized zones which are rich in Iron ore (TM image. Ratio 5/4).

SPATIAL DISTRIBUTION OF THE IRON MINES IN THE STUDY AREA

The **(Figure, 11)** shows the more favorable zones of Iron Bearing Formation, besides the potentially mineralized zones which are rich in Iron ore.

In the **(Figure, 12)**, is shown a DEM, where is seem the spatial distribution of Iron Bearing Formation. In this we observe that the mines are in the highest places because is in these areas where the concentration of Iron is higher.

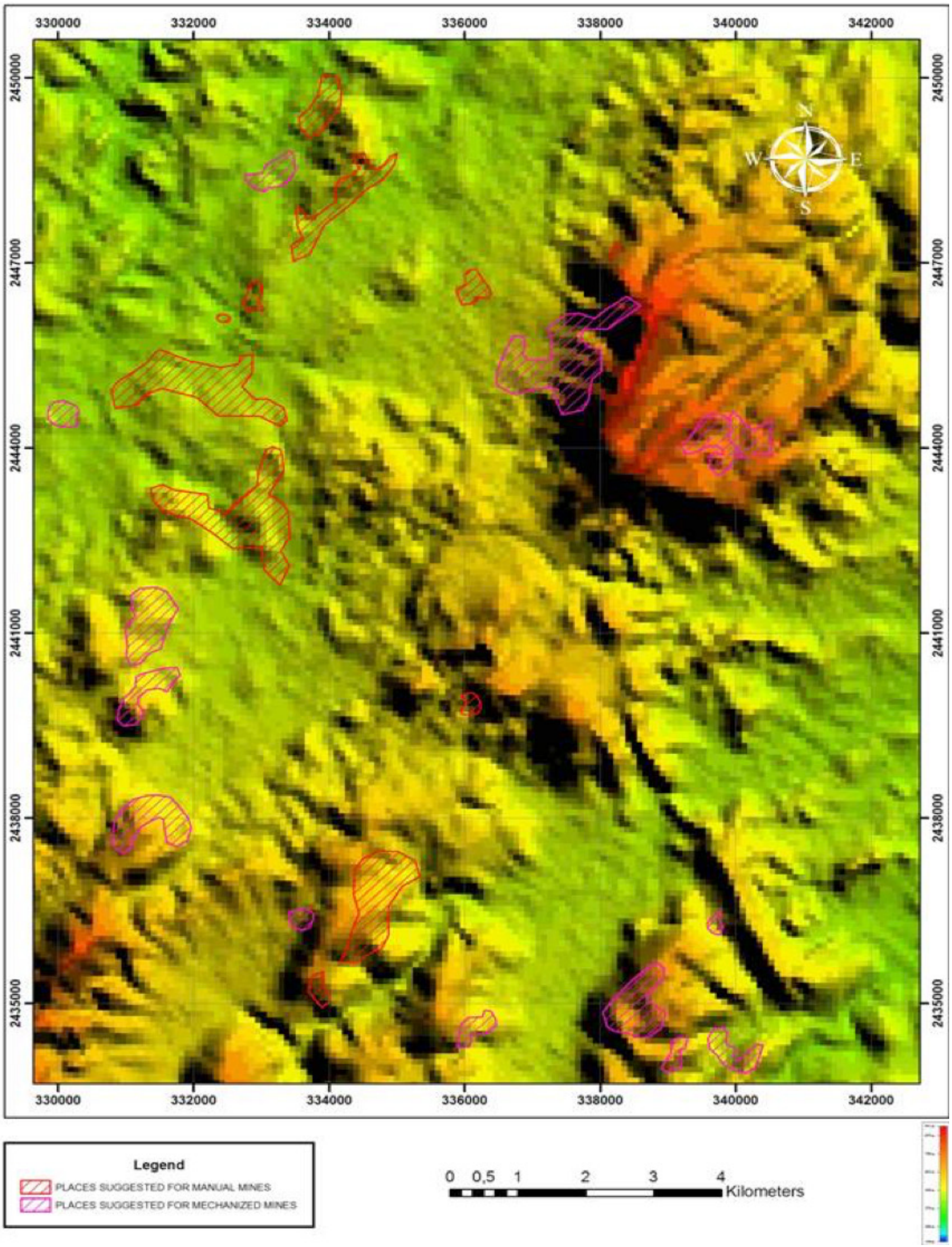

Figure 12. - DEM with the more favorable zones of Iron Bearing Formation and potentially mineralized zones which are rich in Iron ore.

CONCLUSIONS

Image processing and image analysis was done in the spectral and spatial domain with keeping an eye on the objective of our study. Ratio transformations and PC transformations were generated for the analysis of Landsat TM digital data. Ratio 3/1 gave good information about the zones with strong hematitic alteration. The 5/7 ratio was used for identifying clay-rich rocks, besides this ratio was useful for targeting Iron minerals because this have reflectance and absorptions features in these bands. The 5/4 ratio enhanced possible ferrous oxides.

A false colour composite image was generated by combining ratio 5/7, 5/4 and 3/1 in R, G and B respectively. The obtained image mapped the bearing mineral zone (Ferric Zones) in bluish. Another composite image was produced using ratio 3/1, PC2 and Band7 in R, G and B respectively. Although this combination of ratio image appears to be fairly different from the previous one, the final result remains the same thus lending support to the previous conclusion. In the Orissa dataset, all the features other than water and vegetation got highlighted in band rationing as the area has high concentration of iron content due to mining activities.

The first component (PC1) is all positive. This PC1 gave information mainly on albedo and topography. PC2 clearly discriminated the water bodies and mining areas as dark pixels. Analysis of PC3 showed that the most important contributions come from Band 5 (0.167) and Band 7 (0.221). Hydroxyl-bearing (clay) minerals image was obtained by using eigenvector loadings of PC3. The similar analysis of PC4 showed that the most important contributions come from Band 4 (0,299), Band 5 (-0.732) and Band 7 (0.607). Based on spectral characteristics of iron oxide, it follows that iron oxide will be mapped by bright pixels and ferrous minerals in dark grey. Iron oxide image was obtained by using eigenvector loadings of PC4. PC5 contains positive information from band 7 (0.109) and negative information from band 3 (-0.687) which showed the position of hydroxyl ions as dark-gray pixels. PC6 mostly showed noise in the dataset, limiting the use particular of this particular band in our analysis.

For the hyperspectral analysis, endmembers were selected after understanding the geology of the study area. Three endmembers were selected for Orissa. The number of endmembers selected also depends upon the mapping technique used. Linear spectral Unmixing technique requires all the land use classes to be included to give a better result. After collection of endmembers they are used in various mapping techniques.

Mapping technique such as Linear Spectral Unmixing and Mixture Tune Matched Filtering were used to map the different endmembers for Orissa study area. The three endmembers used for the Orissa study area are Hematite, Minetailings and Alluvium. The Linear Spectral Unmixing method successfully mapped the hematite and alluvium. The MTMF method was adopted for the Orissa study area primarily to differentiate between the hematite mineral and minetailings. The MTMF successfully conducted the abundance mapping for hematite and minetailing. The final interpretations of the MTMF results need to be done after integrating the score image results to that of the infeasibility image for all the endmembers.

Various mapping techniques have been employed in this study. Linear Spectral Unmixing and Mixture Tune Matched Filtering are few of the techniques that have been used. A single mapping technique has not given all the endmember classified result. In the case of Orissa study area, Linear Spectral Unmixing as well as Mixture Tune Matched Filtering has given good results. Hence it can be concluded that an integrated approach of several mapping techniques will lead to the successful mapping of the endmembers. The great concentrations of Iron are in the mines that are placed in the highest zones.

REFERENCES

BAKLIWAL, P.C. AND RAMASAMY, S. M. (1987). Lineament fabric of Rajasthan and Gujarat, India, Rec. Geol. Surv. Ind., v.113 (7), pp. 54-64.

BOARDMAN, J.W. (1989). Inversion of Imaging Spectrometry data using singular value decomposition (abs): in proceedings, IGARSS'89, 12 Canadian Symposium on Remote Sensing, Vol. 4.

BOARDMAN, J.W. (1993). Automated spectral unmixing of AVIRIS data using convex geometry on concepts in summaries (abs). Fourth JPL Airborn Geosciences Workshop, JPL Publication 95-26.

BOARDMAN, J.W., KRUSE, F.A. (1994). Automated spectral analysis: A geologic example using AVIRIS data, north Grapevine Mountains, Nevada: in proceedings, Tenth Thematic conference on geologic remote sensing, Environmental research institute of Michigan, Ann Arbor.

BOARDMAN, J.W., KRUSE, F.A., AND GREEN, R.O. (1995). Mapping target signatures via partial unmixing of AVIRIS data in summaries (abs), Fifth JPL Airborn Earth Science Workshop, JPL publication 95-1.

CLARK, R.N., KING, T., KLEJWA, M. AND SWAYZE, G.A., 1990. High spectral resolution reflectance spectroscopy of minerals. Journal of Geophysical research 95 (B8): 653-680.

CUDAHY AND IN PAPP, E., 2002 Geophysical and Remote Sensing Method for Regolith Exploration CRCLEME Open File Report 144, pp 13-21.

DATT, B., MCVICAR, T.R., VAN NIEL, T.G., JUPP, D.L.B. AND PEARLMAN, J.S., 2003. Preprocessing EO-1 Hyperion hyperspectral data to support the application of agricultural indexes. IEEE Transactions on Geoscience and Remote Sensing, 41(6 Part 1): 1246-1259.

DUNN, J.A., (1940). The stratigraphy of South Singhbhum. Mem. Geol. Surv. Ind., V 63, pt. 3.

GOODENOUGH, G.D., DYK, A., NIEMANN, O.K. AND PEARLMAN, J.S., 2003. Preprocessing Hyperion and ALI for forest classification. IEEE Transactions on Geoscience and Remote Sensing, 41(6 Part 1): 1321-1331.

GROSS, H.N. AND SCHOTT, J.R., 1998. Application of Spectral Mixture Analysis and Image Fusion Techniques for Image Sharpening. Remote Sensing of Environment, 63(2): 85-94.

GRIFFIN, M.K. AND HSIAO-HUA, K.B., 2003. Compensation of Hyperspectral data for atmospheric effects. Lincoln Laboratory Journal, 14(1): 29-53.

GUPTA *et al.* (1981). Lithostratigraphic map of Aravalli region, Southeastern Rajasthan and northern Gujarat, Geol. Surv. Ind., Hyderabad.

HARSANYI, J.C., CHANG, C., 1994. Hyperspectral image classification and dimensionality reduction: An Orthogonal subspace projection approach. IEEE Transactions on Geoscience and Remote Sensing 32, 779-785.

Hunt, G.R., Salisbury, J.W. and Lehnoff, C.J., 1971. Visible and near infrared spectra of minerals and rocks: 111. Oxides and Oxyhydroxides. Modern Geology 2: 195-205.

JANSSEN, L.L.F., WEIR, M.J.C., GRABMAIER, K.A. AND KERLE, N., 2004. Geometric aspects. In: N. Kerle, L.F.L. Janssen and G.C. Huurneman (Editors), Principles of remote sensing. ITC education text book series. The international institute for geo-information science and earth observation (ITC), Enschede, pp. 317-345.

JONES, H.C. (1934) – The Iron ore deposits of Bihar and Orissa. Mem_Geological Survey of India Vol. 63 pp. 2.

JUPP, D.L.B., DATT, B., LOVELL, J., CAMPBELL, S. AND KING, E., 2004. Backgroung notes for Hyperion data user workshop, CSIRO office of space science and applications, Earth Observation Centre.

KRUSE, F.A., KIEREINYOUNG, K.S. AND BOARDMAN, J.W., 1990. Mineral Mapping at Cuprite, Nevada with a 63-Channel Imaging Spectrometer. Photogrammetric Engineering and Remote Sensing, 56(1): 83-92.

KRUSE, A.FRED., 2002. Comparison of AVIRIS and Hyperion for Hyperspectral Mineral mapping.

KRUSE, F.A., BOARDMAN, J.W. AND HUNTINGTON, J.F., 2003b. Final Report: Evaluation and Geologic Validation of EO-1 Hyperion, NASA.

LILLESAND, T.M. AND KIEFER, R.W., 1999. Remote Sensing and Image Interpretation. John Wiley & Sons, Inc, 9-10, 592-597 pp.

MATTHEW, M.W. *et al.*, 2000. Status of atmospheric correction using a MODTRAN4-based algorithm, Algorithms and Technologies for Multispectral, Hyperspectral, and Ultraspectral Imagery VI. SPIE, Orlando, FL, USA.

MATTHEW, M.W. *et al.*, 2000. Status of atmospheric correction using a MODTRAN4-based algorithm, Algorithms and Technologies for Multispectral, Hyperspectral, and Ultraspectral Imagery VI. SPIE, Orlando, FL, USA.

MURTHY, V.N. AND ACHARYA, S. (1975) – Lithostratigraphy of the Preccambrian rocks around Koira, Orissa, Jr. Geol. Soc. Ind. Vol 16 (1) pp 55-68.

PANTAZIS, M. *et al.*, 1998. Trade Studies in Multi/ hyperspectral Imaging Systems Final Report.

RAMSEY, E. AND NELSON, G., 2005. A whole image approach using field measurements for transforming EO1 Hyperion hyperspectral data into canopy reflectance spectra. International Journal of Remote Sensing, 26(8): 1589-1610.

ROBILA, S.A. AND GERSHMAN, A., 2005. Spectral matching accuracy in processing hyperspectral data. IEEE Transactions on Geoscience and Remote Sensing, 1(1): 163- 166.

ROY, S.-S., MALHOTRA, G. AND MOHANTY, M., 1998. Geology of Rajasthan. Geological Society of India, Balgalore, 278 pp.

SABINS, H.F. – Remote sensing, Principles amd interpretation edition (Text) pp 177 – 233.

SARKAR, S.N. AND SAHA, A.K. (1977) – The present status of the Precambrian stratigraphy, tectonic and geochronology of Singhbhum, KJR-Mayurbhanj region, eastern India, Ind. Jr. Earth Sc. Pp 37-65.

SARKAR, S.N AND SAHA, A.K. (1983) – Structure and tectonics of the Singhnhum Orissa Iron Ore craton, Eastern India, Recent researches in Geology, Vol 10, pp 1-18.

SINHA-ROY, S. (1988). Proterozoic Wilson Cycles in Rajasthan. In : A.B. Roy (Eds) Precambrians of Aravalli Mountain, Rajasthan, India, Mem, Geol. Soc. Ind. V. 7, pp. 95-105.

VAN DER MEER, F., 2004. Analysis of spectral absorption features in hyperspectral imagery. International Journal of Applied Earth Observation and Geoinformation, 5(1): 55-68.

VAN DER MEER, F., 2006. The effectiveness of spectral similarity measures for the analysis of hyperspectral imagery. International Journal of Applied Earth Observation and Geoinformation, 8(3): 3-17.

OTHER REFERENCES:

http://glovis.usgs.gov/

http://geo.arc.nasa.gov/sge/health/sensor/sensors/irsp6.html

http://www.csr.utexas.edu/projects/rs/hrs/hyper.html

http://speclab.cr.usgs.gov/spectral.lib456.descript/DESCRIPT/quartz.avent.hs117.html